InSight: Using Earth data to demonstrate inversion techniques for Mars’ interior

Mark P. Panning[1], Antoine Mocquet[2], Eric Beucler[2], W. Bruce Banerdt[3], Philippe Lognonné[4], Lapo Boschi[5], Catherine Johnson[6,7], Renee C. Weber[8]

1. Dept. of Geological Sciences, University of Florida, (mpanning@ufl.edu), 2. Laboratoire de Planétologie et Géodynamique, Université de Nantes, 3. Jet Propulsion Laboratory, California Institute of Technology, 4. Institut de Physique du Globe Paris, 5. Institute of Geophysics, ETH Zurich, 6. Dept. of Earth and Ocean Sciences, University of British Columbia, 7. Planetary Science Institute, Tucson, AZ, 8. NASA Marshall Space Flight Center

1. Introduction

InSight is a proposed Discovery mission which will deliver a lander containing geophysical instrumentation, including a heat flow probe and a seismometer package, to Mars to perform, for the first time, an in-situ investigation of the interior of a truly Earth-like planet other than our own. However, since the mission will have a single lander and no seismic network, we will need to take advantage of single station approaches, and these approaches should be tested with Earth data.

2. Detectability

Using estimates of Martian seismicity based on thermal calculations [1] or visible faulting [2,3], we expect to record body waves for many events greater than or equal to 10^{14}Nm, and on the order of 8 events with seismic moment greater than or equal to 10^{16}Nm (M_W4.7).

Figures 1 and 3 show some example Earth seismograms in this range. Higher orbit surface waves should be easier to detect on Mars due to lower noise and attenuation from absence of oceans, and shorter propagation distances (figure 2), based on synthetics calculated in a model of Martian structure [4].

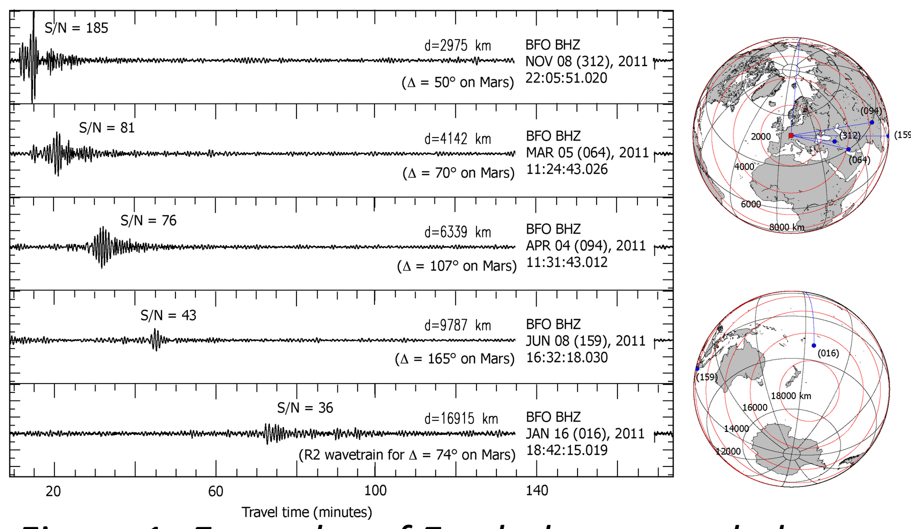

Figure 1: *Examples of Earth data recorded at BFO station for M_W 5.3 events. The equivalent epicentral distances on Mars are indicated.*

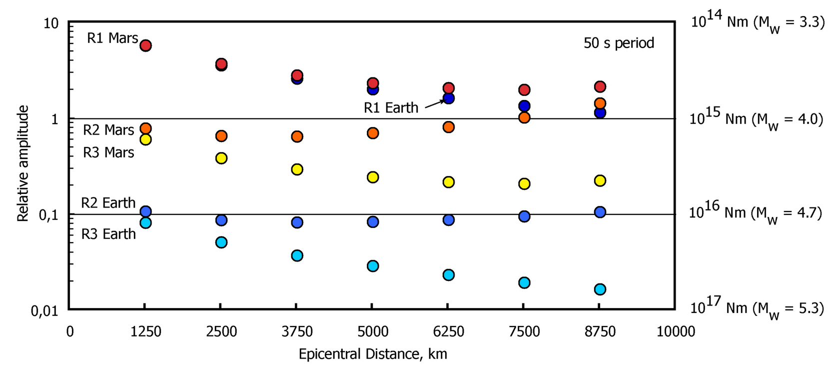

Figure 2: *Amplitude of Rayleigh wave trains normalized by R1 amplitude at an epicentral distance of 10,000 km. S/N numbers on y-axis are for M_W 4, but seismic moment labels on right of figure indicate the minimum amplitude that is required to observe a wave train with a S/N ratio of 1.*

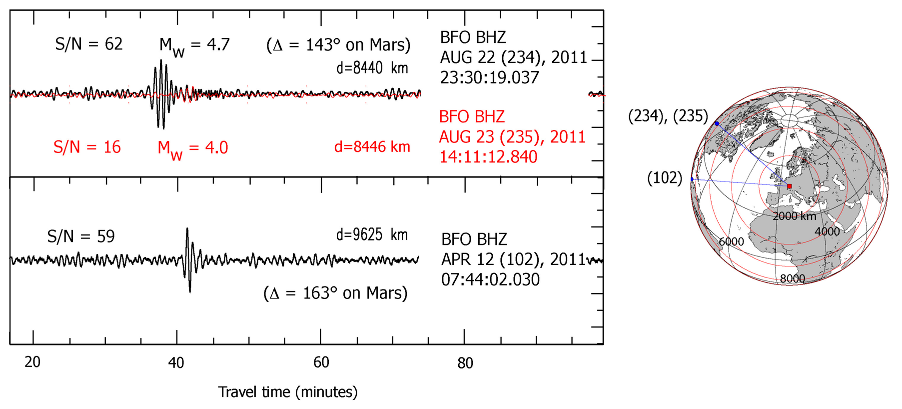

Figure 3: *Same as Figure 1 for M_W 4.0 – 4.7 events.*

3. Single station locations

We estimate location using the timing of 3 orbits of surface waves (e.g. R1, R2, and R3 in figure 4). There are 3 unknowns: Δ, the distance in radians, t_0, the origin time, and v, the surface wave group velocity.

$v=2\pi/(R3-R1)$

$\Delta=\pi-v(R2-R1)/2$

$t0=R1-\Delta/v$

The detectability effects discussed above mean we need events larger by roughly a factor of 100 on Earth, and this study uses events between M_W6 and M_W6.5. Filtering is acausal with 40 second bandwidth, with picks made on data envelopes (fig. 4).

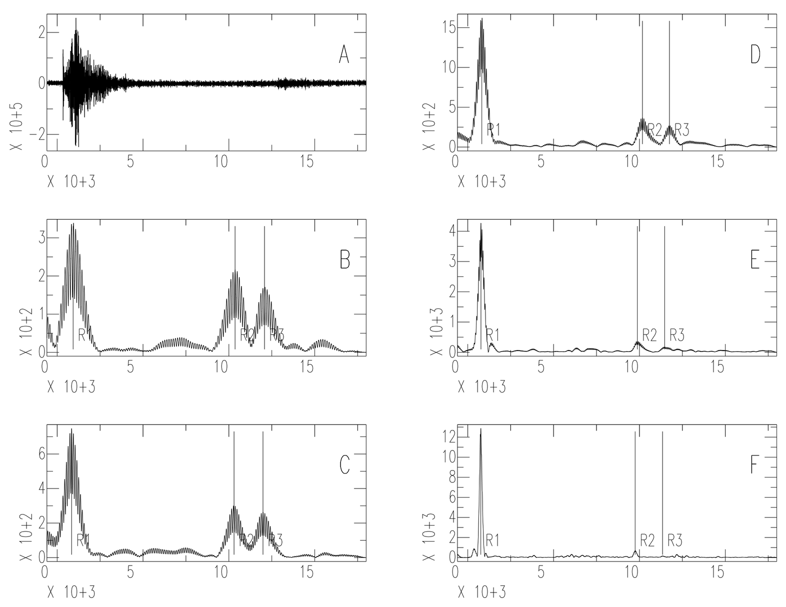

Figure 4: *Example higher orbit surface wave picks for a MW6.1 event recorded on the vertical component of BFO. A is raw data, while B-F show envelopes of passbands centered on 250, 210, 170 130, and 90 seconds.*

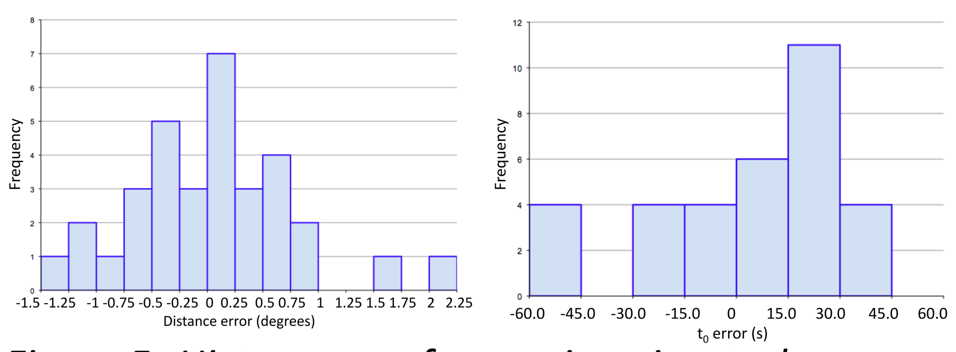

Figure 5: *Histograms of errors in epicentral distance (in degrees, left) and origin time (right) for 33 events between 0° and 90° distance.*

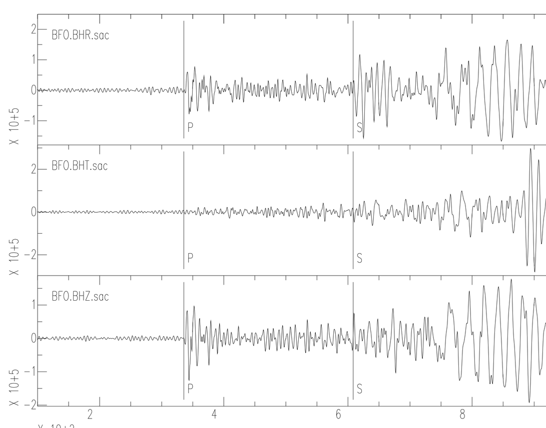

Figure 6: Body wave picks for the event from figure 4.

4. Herglotz-Weichert inversion

Many early 1D models of Earth structure based on travel times utilized Herglotz-Weichert analytic inversion techniques [5], which basically determine velocity structure from the slopes of the best-fit lines through the travel time picks (fig. 7). However, the large errors (fig. 5), including systematically early times between 30 and 60, do not allow for stable results, producing a very high velocity model (the thin red line starting model in figure 8 below).

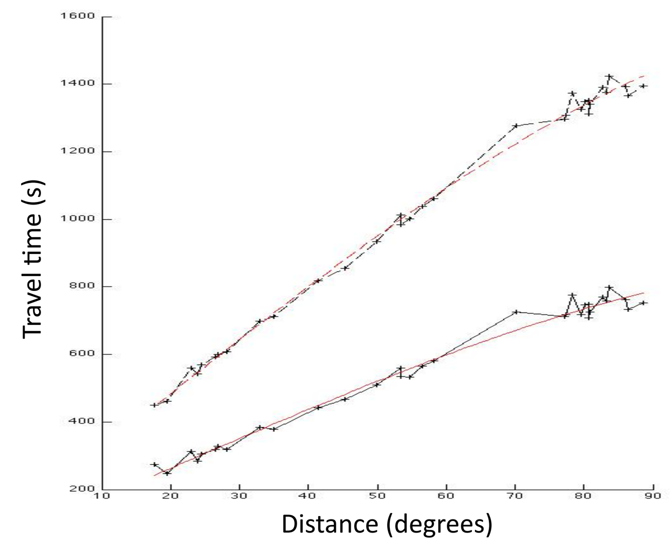

Figure 7: *Constrained monotonic, concave down fits to travel time picks.*

5. Linearized travel time inversion

Stable and accurate models are obtained using a simple linearized inversion scheme based on 1D ray tracing using the *TauP Toolkit* [6]. The models are parameterized with a simple 1 layer 40 km thick crust (to which the data is nearly insensitive), five 400 km thick layers and a 1000 km thick layer below that. Inversion uses Tikhonov regularization, and models are constrained to have non-negative velocity gradients with depth. Velocities are comparable with PREM [7], although somewhat high in the upper mantle, but the change in gradient between upper and lower mantle is clear.

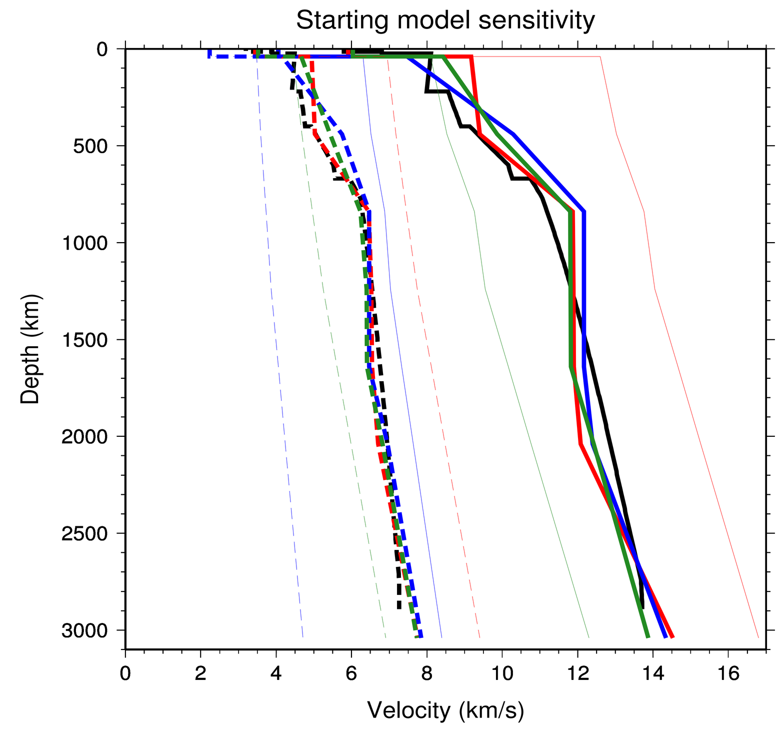

Figure 8: *Starting (thin) and final (thick) models for P (solid) and S velocity (dashed), starting from high (red), low (blue) and moderate (green) initial models. PREM is in black.*

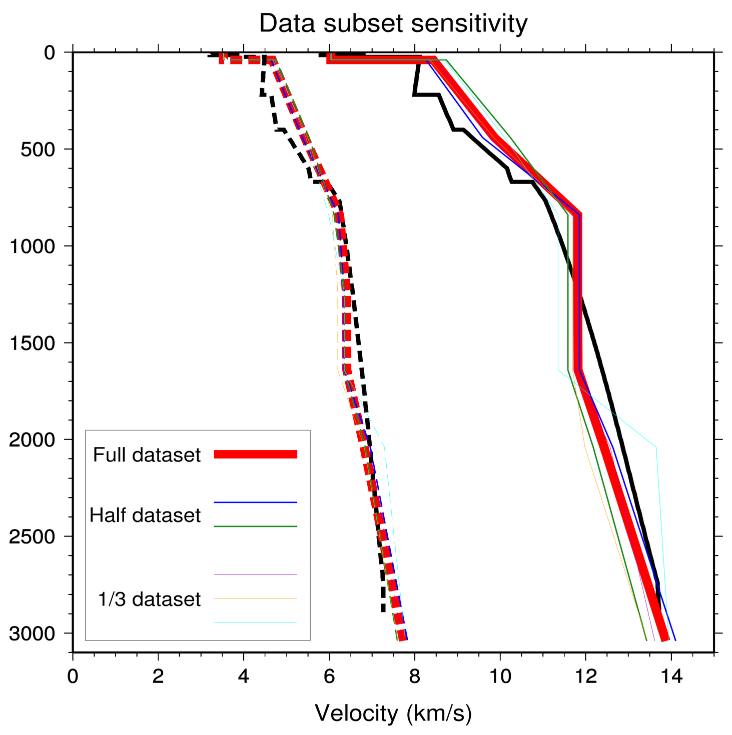

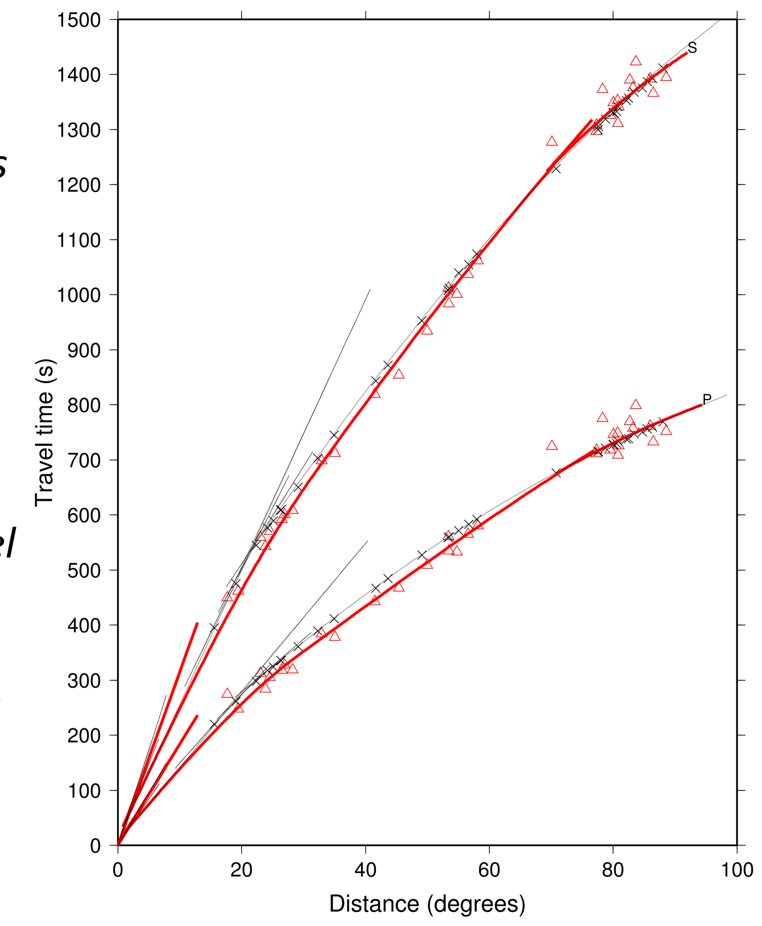

Figure 9 (left): *Inversions subsets of the full 33 event dataset. The full dataset is the thick red line. Inversions of half the dataset (blue and green) and 1/3 the dataset (purple, orange and cyan) are shown.*

Figure 10 (right): *Predicted travel times for the full dataset model (red lines) compared with picks (red triangles), and PREM (black lines) compared with picks referenced to catalog Δ and t_0 (black x’s).*

6. Further work

Additional single station techniques will be important to better constrain structure, particularly in the crust and upper mantle. With 3 orbits of surface waves, great-circle averaged phase velocity dispersion can be recovered [e.g. 8,9] and combined with group velocity estimates from part 3 to better constrain upper mantle structure, while receiver functions [e.g. 10] can be used to constrain crust and upper mantle discontinuities. With better velocity models, smaller events with only P and S picks can also be used.

7. References

[1] R.J. Phillips. Expected rate of marsquakes. In *Scientific Rationale and Requirements for a Global Seismic Network on Mars,* pages 35–38. LPI Tech. Rept., 91-02, Lunar and Planetary Inst., Houston, 1991.
[2] M.P. Golombek, W.B. Banerdt, K.L. Tanaka, and D.M. Tralli. A prediction of Mars seismicity from surface faulting. *Science,* 258:979–981, 1992.
[3] M. Knapmeyer, J. Oberst, E. Hauber, M. Wählisch, C. Deuchler, and R. Wagner. Working models for spatial distribution and level of Mars’ seismicity. *J. Geophys. Res.,* 111:E11006, 2006. doi: 10.1029/2006JE002708.
[4] F. Sohl and T. Spohn. The interior structure of Mars: Implications from SNC meteorites. *J. Geophys. Res*. 102:1613-1635, 1997.
[5] K. Aki and P.G. Richards. *Quantitative Seismology, 2nd edition.* University Science Books, Sausalito, CA, 2002.
[6] H.P. Crotwell, T.J. Owens, and J. Ritsema. The TauP Toolkit: Flexible seismic travel-time and ray-path utilities, *Seism. Res. Lett.* 70:154-160, 1999.
[7] D. Anderson and A.M. Dziewonski. Preliminary reference Earth model. *Phys. Earth Plan. Int.,* 25:297-356, 1981.
[8] Y. Sato. Attenuation, dispersion, and the wave guide of the G wave. *Bull. Seism. Soc. Amer.,* 48:231–251, 1958.
[9] M.N. Toksoz and D.L. Anderson. Phase velocities of long-period surface waves and structure of the upper mantle. *J. Geophys. Res.,* 71:1649–1658, 1966.
[10] R.A. Phinney. Structure of the Earth’s crust from spectral behavior of long-period body waves. *J. Geophys. Res.,* 69:2997–3017, 1964.